DOE/ET/53088-49 IFSR #49

FAST MAGNETIC RECONNECTION PROCESSES

F. Brunel and T. Tajima
University of Texas

and

J. M. Dawson
University of California, Los Angeles

January 1982

Fast Magnetic Reconnection Processes

F. Brunel and T. Tajima

Institute for Fusion Studies

University of Texas

Austin, Texas 78712

and

J. M. Dawson

Department of Physics

University of California

Los Angeles, California 90024

We find through theory and MHD particle simulation that fast magnetic field-line reconnection may consist of more than one stage. After the Sweet-Parker phase establishes for an Alfven time, a faster "second phase" of reconnection takes over if the plasma is compressible: the reconnected flux varies as $\psi = \psi_0 t^{\rho_i/\rho_e}$, where ρ_e and ρ_i refer to the plasma densities outside and inside of the current channel.

Fast magnetic field-line reconnection is a prerequisite to formation of a compact plasma toroid.[1-4] This process was observed in the simulation of a reversed theta-pinch at the island stage, but also at the island destruction stage once the tilting instability sets in.[5] A fast reconnection process is again responsible for destruction of the reversed z-pinch[6] as well as for Kadomtsev's model[7,8] for tokamak disruption. Rapid reconnection is also believed to play an important role in the magnetosphere, the sun's dynamo etc. From our studies by magnetohydrodynamic (MHD) particle simulation and subsequent theoretical development, we found some general characteristics of nonlinear evolution of fast reconnection and we report, in particular, discovery of multiple phases for this process.

Computer simulation has been carried out on a 2 1/2 dimensional MHD particle code[9] with the Lax-Wendroff algorithm to advance the magnetic field. Initially, homogeneous magnetic fields in the x-direction are embedded in a plasma with opposite senses in the lower and upper halves. In order to make the physics simpler, we let the layer between the two regions with reversed fields (i.e. $|y| \leq a$) contain a high density uniform plasma and no magnetic field with sharp boundaries (Similar results have been obtained with smooth boundaries.). The system is bounded in the y-direction with perfect conductors and satisfies the perpendicular pressure equilibrium, until we pinch the plasma locally by one (or two) external current rod(s) normal to the x-y plane (in the z-direction). Figure 1(a) shows an early stage of magnetic fields pinched by one rod.

As the external current pinches the plasma, the magnetic field lines as well as the high density plasma slab are pinched downward [Figure 1(a)]. The perpendicular pressure balance is increased in the region close to the current rod and becomes nonuniform along the column; the plasma in the layer is drawn away from the region of the rod along the field lines. As the plasma flows out, the thickness of the layer decreases exponentially in time,[10] while the local density in the layer remains high. In ideal MHD, the plasma layer develops into a singular current sheet, in a quasi-stationary state, always out of equilibrium.[11]

For resistive (or non-ideal MHD) plasmas, however, the layer width becomes stabilized as field lines begin reconnecting at such a rate that the perpendicular inflow of particles into the current sheet due to the field-line annihilation matches the plasma endloss along the magnetic field lines (see Fig. 1(c)) due to the parallel pressure drop. The inflow is governed by magnetic diffusion due to resistivity in the layer. This is a slow process (although certainly faster than the Rutherford process in the equilibrium) described earlier by Sweet and Parker.[12] We quantify this process by the succeeding analysis.

The in-the-plane magnetic flux ψ and out-of-the-plane (along the z-axis) magnetic field B_z are described by

$$\frac{\partial \psi}{\partial t} + \underset{\sim}{v} \cdot \underset{\sim}{\nabla}\psi = \eta \nabla^2 \psi \tag{1}$$

$$\frac{\partial B_z}{\partial t} + \underset{\sim}{\nabla} \cdot \underset{\sim}{v} B_z = \eta \nabla^2 B_z \tag{2}$$

where $\underset{\sim}{B} = \underset{\sim}{B}_{\perp} + B_z \underset{\sim}{e}_z$ and $\underset{\sim}{B}_{\perp} = \underset{\sim}{\nabla}\psi \times \underset{\sim}{e}_z$; v_z is neglected. For the initial configuration we assume the flux function linearly increasing in y, $\psi = B_e|y|$, on each side of the exteriors of the current sheet located at y=0; this is equivalent to assume a uniform magnetic field of magnitude B_e but as shown in Fig. 1(c). In these exterior regions the diffusion terms are negligible and the flux velocity is determined by the fluid in the y-direction:

$$v = \dot{\psi}/B_e \quad . \tag{3}$$

Inside of the current sheet with half width a, the perpendicular velocity v is zero and the diffusion process becomes important:

$$\dot{\psi} = \eta\nabla^2\psi \simeq \eta B_e/a \quad . \tag{4}$$

The perpendicular inflow of plasma into the current layer over length 2L, $\partial N_{in}/\partial t = 4\rho_e vL$, is equal to the outflow along the field line in the x-direction with velocity u, $\partial N_{out}/\partial t = 4\rho_i ua$. This yields the relation

$$\rho_e vL = \rho_i ua \quad , \tag{5}$$

where subscripts e and i refer to the external and internal quantities with respect to the current sheet. Equations (3) and (5) give

$$\dot{\psi} = B_e u\rho_i a/\rho_e L \quad , \tag{6}$$

while (4) and (5) yield

$$a = \eta^{1/2}(\rho_e L/\rho_i u)^{1/2} \quad . \tag{7}$$

The peak density ρ_i with respect to ρ_e is determined by the perpendicular pressure balance $p_i + B_{iz}^2/8\pi = p_e + B_{ez}^2/8\pi + B_{e\perp}^2/8\pi$. The plasma slab develops a diffuse profile as it becomes thinner as shown by (4). Thus ρ_i in (5) and thereafater is the average density over the slab cross-section. The flow velocity u at the current sheet extremities (or cusps) is determined by the parallel pressure balance $\rho_{ic}u^2/2 = P_{io} - P_{ic} \simeq (B_{\perp eo}^2 - B_{\perp ec}^2)/8\pi$, where the subscripts o and c denote the central and cusp regions, and P_i is the total internal pressure $P_i = p_i + B_{iz}^2/8\pi$. In writing the second equality, we have assumed that the external plasma pressure p_e and "z-direction" magnetic pressure $B_{ez}^2/8\pi$ are nearly uniform, since they equilibrate quickly over the magnetosonic wave transit time. When the cusp field $B_{\perp ec}$ can be neglected in the comparison with $B_{\perp eo}$, we obtain the reconnecting flux velocity as

$$v = R_m^{-1/2}\, c_{Ae}(\rho_i/\rho_e)^{1/2} \quad , \tag{8}$$

where the magnetic Reynolds number $R_m = c_{Ae}L/\eta$ and the Alfven velocity $c_{Ae} = (B_{\perp eo}^2/4\pi\rho_e)^{1/2}$. Sweet and Parker[11] gave an incompressible version ($\rho_i = \rho_e$) of (8).

If the plasma is compressible, however, the poloidal flux reconnected in the Sweet-Parker phase may pile up in the current sheet as time goes on. The current sheet then becomes tapered, shortening the effective exhaust distance L. It is at this stage when a drastic enhancement in the reconnection rate is observed in our simulation [see Figure 1(b)]. A simplified model of this stage may be depicted as in Figure 2(a). The trapped reconnected flux has a tapered structure with pitch angle $\alpha \ll 1$. The new exhaust length L^* is established beyond which a large plasma pressure drop takes place; it corresponds to the point where a critical amount of reconnected flux $\psi_c = aB_e$ is trapped [see Figure 2(a)]. Since the trapped flux varies linearly for $0 < |x| < ut$, we obtain $L^* = L_t\psi_c/\psi$ with $L_t = L^* + ut$, or

$$L^* = ut\psi_c/(\psi-\psi_c) \quad . \tag{9}$$

In the evaluation of L_t we assume that the flux in the current sheet is carried instantly over a distance L^* where diffusion is predominant, and then remained trapped with the fluid which move with a velocity u along x. The width a^* of the reconnected region at $x=L^*$ is 2a, because $a^* = a+\alpha L^*$ where $\alpha = B_y/B_e = \psi/L_tB_e$: a large pressure drop is thus expected since the plasma flow along the field line. The outflow velocity is the area wave velocity[9] $u \simeq c_A$. Once L^* becomes shorter than L, substitution of (9) into (6) yields $t\dot{\psi} - (\rho_i/\rho_e)\psi = -\psi_c$ or

$$\psi = \psi_0(t/t_0)^{\rho_i/\rho_e} + (\rho_e/\rho_i)\psi_c \quad . \tag{10}$$

where $\psi > \psi_c$ after $t_0 \simeq L/u$. If the plasma is compressible, the reconnection rate becomes much faster than that in the Sweet-Parker

phase after t_0 with a shrinking current sheet L^*. There will be a sharp increase in the reconnection velocity given by $v = \dot{\psi}/B_e \propto t^{\delta}$, with $\delta = \rho_i/\rho_e - 1$. We shall call this stage of faster reconnection the second phase. If the plasma is incompressible ($\rho_i = \rho_e$), the Sweet-Parker phase lasts beyond t_0. Correspondence to relations (9) and (10) can be found in our simulation in Figures 1(a) and (b) for shrinking L^* and in Figures 2(b) and (c) for two (or more) phases of $\psi(t)$. The exponent obtained from Figure 2(b) for the second phase is 4.0 with $\rho_i/\rho_e \simeq 4.0$ in the simulation and the exponent from Figure 2(c) is 2.9 with $\rho_i/\rho_e \simeq 3.4$; both cases are in good agreement with (10).

The magnetic force that pulls the plasma out of the current sheet in the x-direction contains two terms: one is $\sim \alpha^2 B_e^2/8\pi a$ due to the curvature of B_y and the other is the x-component of the perpendicular magnetic pressure $F_m = \alpha B_e^2/8\pi\tilde{a}$ considered by Petschek,[12] where $\tilde{a}(x)$ is the local column width. The latter is much larger than the former and is of the same order of magnitude as the parallel plasma pressure drop F_p considered here. Because $\alpha = a/L^*$ and $B_e^2/8\pi = p_i - p_e$, the term F_m is about $(a/\tilde{a})F_p$, and it is large for $|x| < L^*$ where $\tilde{a} \simeq a$. It is noted, however, in our simulation that the plasma flows along the field lines as assumed by us, but not along the x-direction as in Ref. 12. It is also noted that the Petschek term F_m is largely canceled by the pressure term $\alpha(p_i - p_e)/\tilde{a}$.

The geometry of the system is important both for the second phase and for the eventual saturation of reconnection. When the current layer is pinched from both sides so that it remains straight during the reconnection process, a different exponent for the time dependence for the reconnected flux is observed in the second phase. Figure 1(d) shows the flux lines in this case. The rate of reconnection in this case is given in Figure 2(d): $\psi \simeq (t-t_0)^{\xi}$ where $\xi \simeq 2$.

In this latter case we propose the following mechanism which impedes the process (10). In slab geometry field lines due to the combination of a dipole (B_d on axis) and uniform B_e are approximately described by

$$y(x) = y_0(1 + \Theta x^2/r_d^2) \quad , \tag{11}$$

where $|y| \ll r_d$ (close to the plane of symmetry). Here $\Theta = B_d/(B_d + B_e)$ and $2r_d$ is the dipole distance. In this geometry the flux is packed in such a way that the reconnected flux $\psi \lesssim B_e y(x)$ with $x = L_t \sim ut$, where the field line $y(0) = a$ is considered. Using these conditions in (11), we obtain

$$\psi \simeq aB_e\Theta(ut)^2/r_d^2 \quad . \tag{12}$$

If $\psi > B_e y(x)$, the field line would be pushed away, increasing the current sheet thickness and therefore stopping the diffusion and reconnection process. The reason this process (12) is slower than (10) is that when we pinch from both sides, the reconnected field lines close to the current sheet (which is the plane of symmetry for this

case) stay straighter and open up less angle. Equation (12) agrees well with simulation results [Fig. 2(d)].

Finally, previous simulation investigations are consistent with our theory and simulation. Sato and Hayashi's simulation[14] (their Figure 1) shows fast reconnection sets in when L^* becomes the length of their system, consistent with the present theory of the second phase. W. Park's work[8] notes that the incompressible case stays in the Sweet-Parker phase all the way. In the island coalescence process, this second phase of fast coalescence should also exist in the small η case described by Biskamp et al.[15] if the plasma is compressible. Our particular model is one of many[5,6,7,8,14,15] which gives rise to a current singularity (It corresponds to the set-up in Ref. 5 to initiate island formation in a reversed pinch.). However, the model and its subsequent physics are general enough to pertain to many other cases, since nonlinear developments are common over many situations, e.g. the external driven pinch reconnection, the development of the internal coalescence instability, etc.

This work was supported by the Department of Energy Grant DE-5G05-80ET-53088 and by the National Science Foundation Grants PHY80-26048 and ATM81-10539.

References

1. M. Alfven, L. Lindberg, and P. Mitlid, J. Nucl. Energy, Part C 1, 116(1960).

2. J. H. Irby, J.F. Drake, and H.R. Griem, Phys. Rev. Lett. 42, 228(1979).

3. T.R. Jarboe, I. Henins, H.W. Hoida, R.K. Linford, J. Marshall, D.A. Platts, and A.R. Sherwood, Phys. Rev. Lett. 45, 1264(1980).

4. W.C. Turner, et al., Lawrence Livermore Laboratory Report UCRL-85122(1980).

5. F. Brunel and T. Tajima, Bull. Amer. Phys. Soc. 25, 884(1980).

6. E.J. Caramana and D.D. Schnack, Sherwood Theory Meeting paper 3B38(1981).

7. B.B. Kadomtsev, Fiz. Plazmy 1, 710(1975) [Sov. J. Plasma Phys. 1, 389(1975].

8. W. Park, Bull. Amer. Phys. Soc., 26, 845(1981).

9. F. Brunel, J.N. Leboeuf, T. Tajima, J.M. Dawson, M. Makino and T. Kamimura, J. Comp. Phys., 43, 268(1981).

10. F. Brunel, T. Tajima, J.N. Leboeuf, and J.M. Dawson, Phys. Rev. Lett. 44, 1494(1980).

11. S.I. Syrovatskii, Zh. Eksp. Teor. Fiz., 60, 1727(1971) [Sov. Phys. JETP 33, 933(1971)].

12. E.N. Parker, Ap. J. Suppl. Ser. 77, 177(1963).

13. H.E. Petschek, in Symposium on the Physics of Solar Flares, edited by W.N. Hess (NASA, Washington, D.C., 1964), 1964), p. 425.

14. T. Sato and T. Hayashi, Phys. Fluids 22, 1189(1979).

15. D. Biskamp and H. Welter, Phys. Rev. Lett. 44, 1069(1980).

Figure Captions

Figure 1 - Flux lines ψ. (a) One-pinch case in the Sweet-Parker phase (t=30) and (b) the second phase (t=75), where L^* is indicated ($L^* = x^* - x_0$). (c) Sweet and Parker model for reconnection. (d) Two-pinch case in the second phase (t=75), where L^* and L_t($L_t = x_t - x_0$) are shown. t is in unit of Δ/c_s, where Δ is the grid spacing in y and c_s the sound speed.

Figure 2 - (a) Model for "second phase". (b)-(d) Log-log plots of ψ vs. t. (b) One-pinch case with resistivity $\eta = 0.01$. Line 1 has a slope 0.86 and line 2 has 4.0. (c) One-pinch case with $\eta = 0.1$. Line 1 has slope 1.0 and line 2 has 2.9. (d) Two-pinch case $\eta = 0.1$ with slope 1.8 in unit of $c_s\Delta$. We have defined $x^* = x_0 + L^*$ and $x_t = x_0 + L_t$.

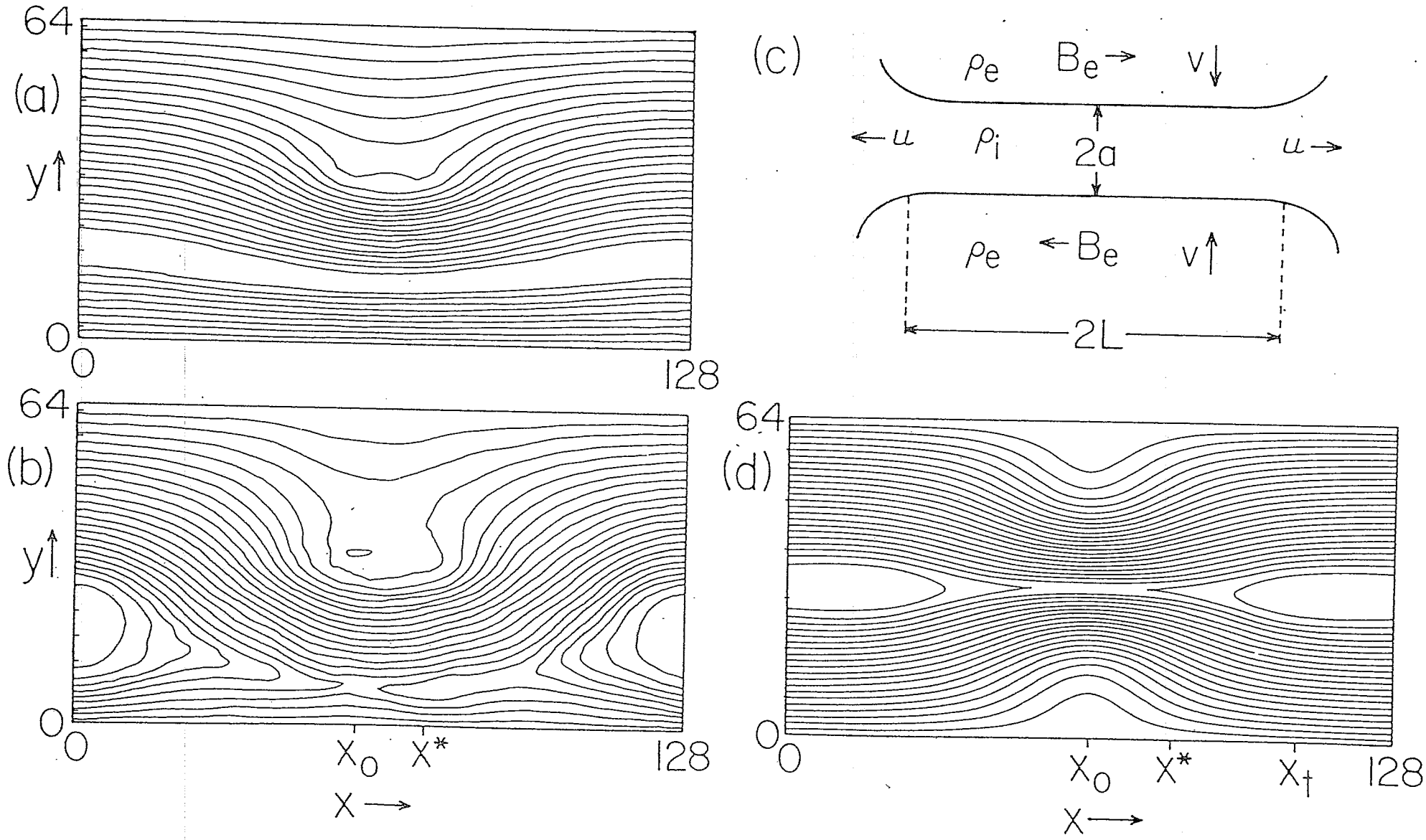
64
(a)
y
0
0
128
(c)
ρ_e B_e v
u
ρ_i
2a
u
ρ_e B_e v
2L
64
(b)
y
0
0
X_0 X^*
128
X
64
(d)
0
0
X_0 X^* X_t 128
X

FIG. 1

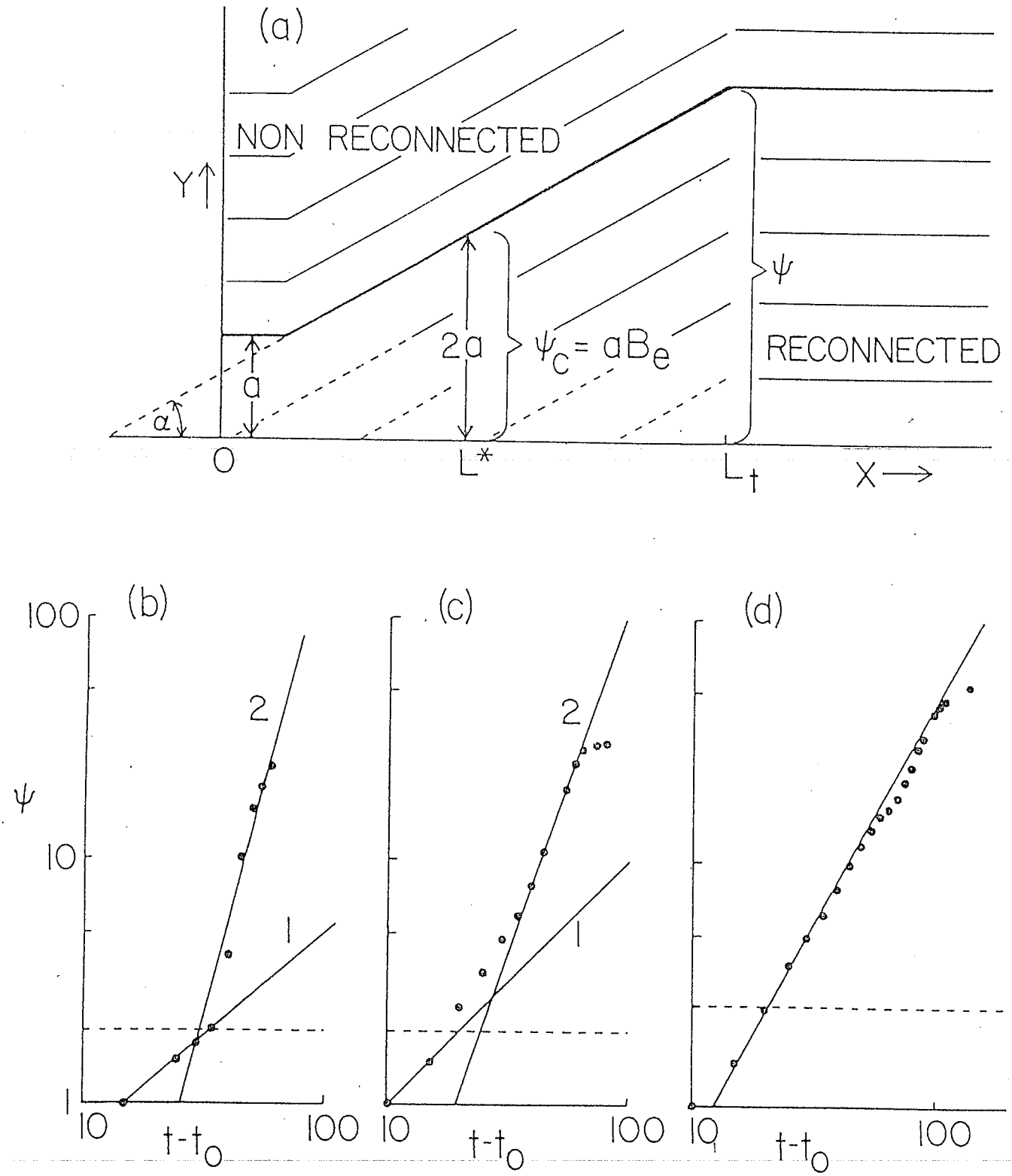
(a)
NON RECONNECTED
Y
ψ
2a
$\psi_c = aB_e$
RECONNECTED
a
α
0
L*
L_t
X
(b)
(c)
(d)
100
10
1
ψ
2
1
10
100
$t-t_0$

FIG. 2